SUPPLEMENTARY INFORMATION

Molecular Origin of Donor- and Acceptor-rich Domain Formation in Bulk-heterojunction Solar Cells with an Enhanced Charge Transport Efficiency

Guankui Long,[†,‡] Rui Shi,[§,=,‡] Yecheng Zhou,[⊥] Ailin Li,[//] Bin Kan,[†] Wei-Ru Wu,[▽,○] U-Ser Jeng,[▽,○] Tao Xu,[◆] Tianying Yan,[//] Mingtao Zhang,[†] Xuan Yang,[†] Xin Ke,[†] Litao Sun,[◆] Angus Gray-Weale,[⊥] Xiangjian Wan,[†] Hongtao Zhang,[†] Chenxi Li,[†] Yanting Wang[,§,#] and Yongsheng Chen[*,†]*

‡These authors contributed equally to this work.

[*]Correspondence to: wangyt@itp.ac.cn; yschen99@nankai.edu.cn.

[†]State Key Laboratory and Institute of Elemento-Organic Chemistry, Collaborative Innovation Center of Chemical Science and Engineering, School of Materials Science and Engineering, Nankai University, Tianjin 300071, China

[§]CAS Key Laboratory of Theoretical Physics, Institute of Theoretical Physics, Chinese Academy of Sciences, 55 East Zhongguancun Road, P.O. Box 2735, Beijing 100190, China

[=]Department of Fundamental Engineering, Institute of Industrial Science, University of Tokyo, 4-6-1 Komaba, Meguro-ku, Tokyo 153-8505, Japan

[∥] Institute of New Energy Material Chemistry, Tianjin Key Laboratory of Metal- and Molecule-Based Material Chemistry, Collaborative Innovation Center of Chemical Science and Engineering (Tianjin), School of Materials Science and Engineering, Nankai University, Tianjin 300071, China

[⊥]School of Chemistry, University of Melbourne, Parkville, VIC, 3010, Australia

[#]School of Physical Sciences, University of Chinese Academy of Sciences, 19A Yuquan Road, Beijing 100049, China

[▽]National Synchrotron Radiation Research Center, Hsinchu Science Park, Hsinchu 30077, Taiwan

[○]Chemical Engineering Department, National Tsing-Hua University, Hsinchu 30013, Taiwan

[◆]SEU-FEI Nano-Pico Center, Key Laboratory of MEMS of Ministry of Education, Southeast University, Nanjing 210096, China

1. Details of coarse-grained (CG) molecular dynamics (MD) simulations

The multiscale corase-graining (MS-CG)[1, 2] approach rigorously constructs from atomistic MD simulation trajectories the CG force fields for a given molecular system. The all-atom MD simulations were performed by using the *GROMACS* MD simulation package[3-5] with the simulation setup exactly the same as in our previous simulation work.[6] The initial configuration was equilibrated with the constant *NPT* ensemble at a very high temperature T = 1000 K (P = 20 atm) for 5 ns to ensure that the system loses its memory of the initial configuration and achieves equilibration. The equilibrated configuration was then subjected to an annealing process, sequentially cooled from T = 1000 K (20 atm) down to 800 K (20 atm), 600 K (20 atm), 400 K (20 atm), 400 K (10 atm), 400 K (5 atm), 400 K (1 atm), 350 K (1 atm) and 300 K (1 atm). The system was equilibrated for 5 ns at each temperature. The configuration obtained at T = 300 K was equilibrated under the constant *NPT* ensemble (P = 1 atm) for an additional 100 ns. Finally, a production run of 50 ns was performed under the same *NPT* ensemble (P = 1 atm, T = 300 K). A total of 5000 configurations were evenly sampled during the production run with the net force on each atom recorded.

The DL_POLY program (version 2.14)[7] was used to perform the CG MD simulation. The blend systems consist of 131584 $PC_{71}BM$ molecules and 169984 **DERHD7T** or 163840 **DRCN7T** molecules, coincident with the experimental molar ratio between donors and acceptors.[8] The initial configurations were equilibrated with the constant *NPT* ensemble at a very high temperature T = 2000 K (P = 20 atm) for 200 ps to ensure that the system loses its memory of the initial configuration. The last configuration was then subjected to an annealing process, sequentially cooled from T = 2000 K (20 atm) down to 1700 K (20 atm), 1400 K (20 atm), 1100 K (20 atm), 900 K (20 atm), 800 K (20 atm), 700 K (1 atm), 600 K (1 atm), 550 K (1 atm), 500

K (1 atm), 450 K (1 atm), and 400K (1 atm). The system was equilibrated for 150 ps at each temperature. The production run at T = 400 K lasted 1 ns after an equilibration run of 500 ps. Note that the dynamics of the CG MD simulations are at least one order of magnitude faster than the corresponding all-atom MD simulations.

2. Heterogeneity Order Parameters

The *heterogeneity order parameter* (HOP) was initially designed to measure the nanoscale spatial heterogeneity in ionic liquid systems,[9] and later on also applied to quantifying the degree of aggregation of polyglutmine molecules.[10] For a given configuration in this study, the HOP is defined for a certain type of CG sites (e.g., sites A) as:

$$HOP = \frac{1}{N_s}\sum_{i=1}^{N_s}\sum_{j=1}^{N_s}\exp(-r_{ij}^2 / 2\sigma^2) \qquad \text{(S1)}$$

where r_{ij} is the distance between sites i and j corrected with periodic boundary conditions, and $\sigma = L/N_S^{1/3}$. Here, L is the side length of the cubic simulation box and N_S is the total number of a certain type CG sites. According to its definition, closer sites contribute more to the HOP value, so a larger HOP value represents a higher degree of aggregation. The form of **Equation S1** ensures that the HOP is topologically invariant with the absolute size of the simulation box. When the number of sites is very limited, however, the HOP exhibits a finite size effect. To demonstrate this effect, the HOP values for ideally uniform systems with $N_S = n^3$ sites (n=1, 2, 3, ...) in a cubic volume are listed in **Table S1**. It can be seen that the HOP attains its ideal, constant value (15.7496) only for $N \geq 729$.

Table S1. The Heterogeneity Order Parameter for Ideal Uniform Systems Containing N_S Sites.

N_S	HOP
1	1.0000
8	4.1464
27	10.8388
64	12.9513
125	15.3220
216	15.5285
343	15.7368
512	15.7431
729	15.7495
1000	15.7495
1728 and larger	15.7496

3. Binding energy calculation

The molecular structures for all the dimers were optimized by density functional theory (DFT) calculations at the level of *w*B97XD/6-31G*.[11] To simplify the calculations, the octyl groups in the oligothiophene donors were replaced by simpler ethyl groups. All DFT calculations were carried out by using the *Gaussian 09* package.[12]

4. Two dimensional-grazing incidence small-angle X-ray scattering (2D-GISAXS)

For the 2D-GISAXS measurements, the active layers were spin-casted on silicon wafers with pre-coated PEDOT:PSS, and then subject to the similar post treatment as that for the device film (100^{o}C for 10 min). GISAXS measurements were performed at the 23A SWAXS Endstation of the National Synchrotron Radiation Research Center (NSRRC) in Taiwan, using a Pilatus 1M-F area detector for GISAXS.[13] With the sample surface defined in the *x*-*y* plane and the incident X-rays in the *x*-*z* plane, the scattering wavevector transfer $\boldsymbol{q} = (q_x, q_y, q_z)$ can be decomposed into three orthogonal components of $q_x = 2\pi\lambda^{-1}(\cos\beta\cos\phi - \cos\alpha)$, $q_y = 2\pi\lambda^{-1}(\cos\beta\sin\phi)$, and $q_z = 2\pi\lambda^{-1}(\sin\alpha + \sin\beta)$, where α and β stand for the incident and exit angles and φ for the scattering angle away from the *y*-*z* plane; λ is the wavelength of the X-ray. The 10 keV X-ray beam of 0.2 mm diameter was used with a sample incident angle of 0.2°, and the sample-to-detector distance was 5.0 m for the GISAXS measurement.

5. Transmission electron microscopy

The active layers were immersed in DI water for exfoliation and then transferred to a Cu foil for image recording. The TEM (FEI Talos F200X TEM) was operated at 200 keV, with gun lens of 3.6 and TEM spot size of 9. TEM bright-field images were obtained by FEI Talos F200X TEM, which was equipped with the beam-blank function.

6. Percolation-ratio calculation

To quantify the hole and electron transport properties of the two systems, the percolation ratios of both oligothiophene donors and fullerene acceptors to the electrodes were calculated. If the center-of-mass (COM) distance of two fullerene acceptors is less than a threshold value r_c (the diameter of $PC_{71}BM$), these two fullerenes are considered connected; if the distance of any

two inter-molecular CG sites of the neighboring donor molecules is closer than r_c (the first strong RDF peak in Figure 2e and 2f), the two donor molecules are considered connected. The connected acceptors and donors can form large clusters in the space, and a percolated cluster is the one percolating through the simulation box and thus providing transport channels for holes or electrons. A system exhibits better hole (electron) transport properties with more oligothiophene (fullerene) molecules belonging to percolated clusters.

7. Structure factors

The structure factors were computed according to the method used by Margulis *et al*.[14, 15] The total static structure function is calculated from the **Equation (S2)**,

$$S(q) = \frac{\rho_0 \sum_i \sum_j x_i x_j f_i(q) f_j(q) \int_0^\infty 4\pi r^2 \left(g_{ij}(r) - 1\right) \frac{\sin qr}{qr} \mathrm{d}r}{\left[\sum_i x_i f_i(q)\right]^2} \qquad \text{(S2)}$$

where i,j denote the atom type and x_i, f_i are the corresponding atomic fraction and atomic form factor of the specific atom type. In **Equation S2**, ρ_0 is the bulk density and $g_{ij}(r)$ is the corresponding pair distribution functions for the specific pair including atom i and j.

As shown in **Figure S1**, in the smaller simulated box, the finite-size effects are more obvious, and the fullerenes all aggregate together in the smaller box. Based on our experimental studies, the domain size of fullerenes is around 6.88 nm, thus the PBC box of 10.4 nm×10.4 nm×10.4 nm and 20.7 nm×20.7 nm×20.7 nm is not large enough to get the complete information of the morphology in the active layer.

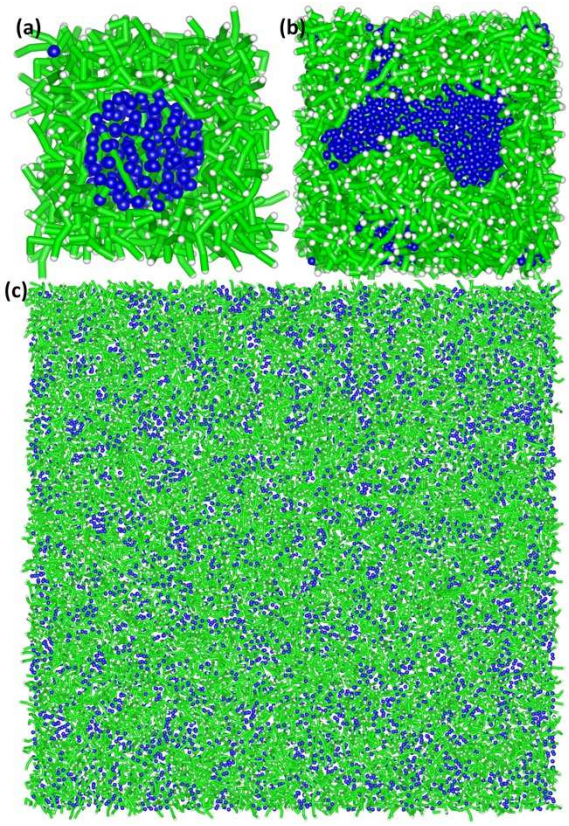

Figure S1. The snapshots of the simulated morphologies for the **DRCN7T**:$PC_{71}BM$ blends with periodic boundary conditions (PBC) applied of ~10.4 nm×10.4 nm×10.4 nm (a), ~20.7 nm×20.7 nm×20.7 nm (b) and ~83 nm×83 nm×83 nm. The oligothiophene chains were colored with green and fullerenes were colored with blue. The snapshots in (a) and (b) were magnified 4 and 2 times to compare the simulated results in (c).

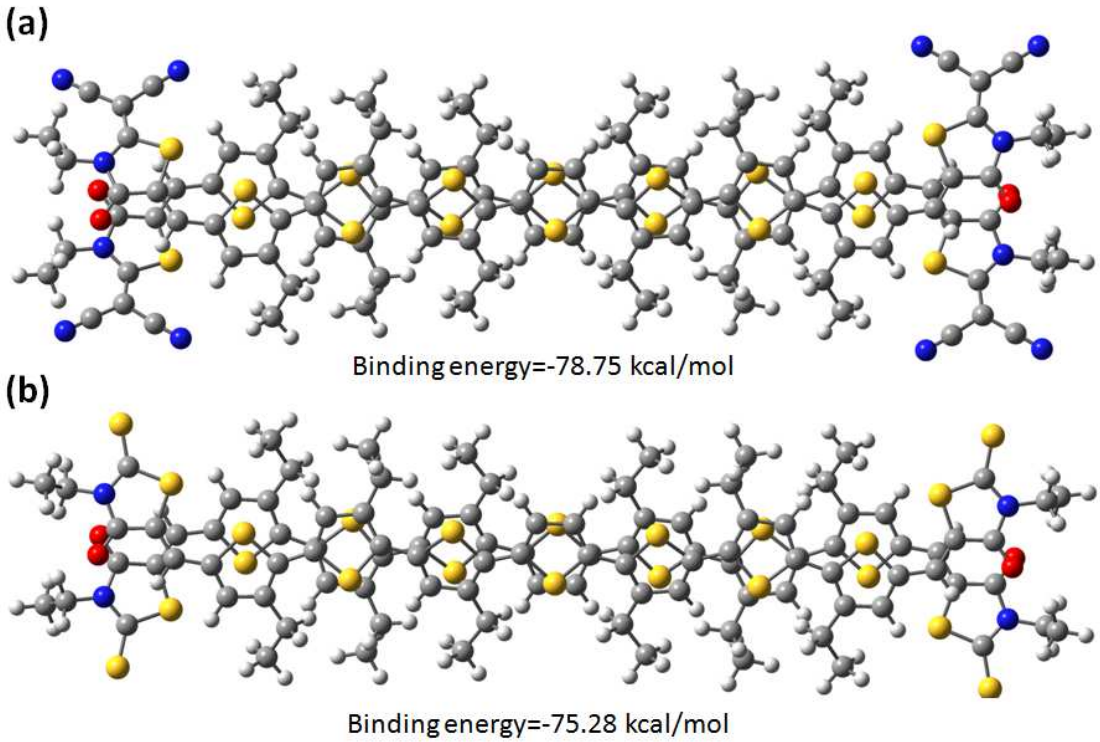

Figure S2. The optimized dimer structures and associated binding energies by DFT calculation for **DRCN7T**:**DRCN7T** (a) and **DERHD7T**:**DERHD7T** (b).

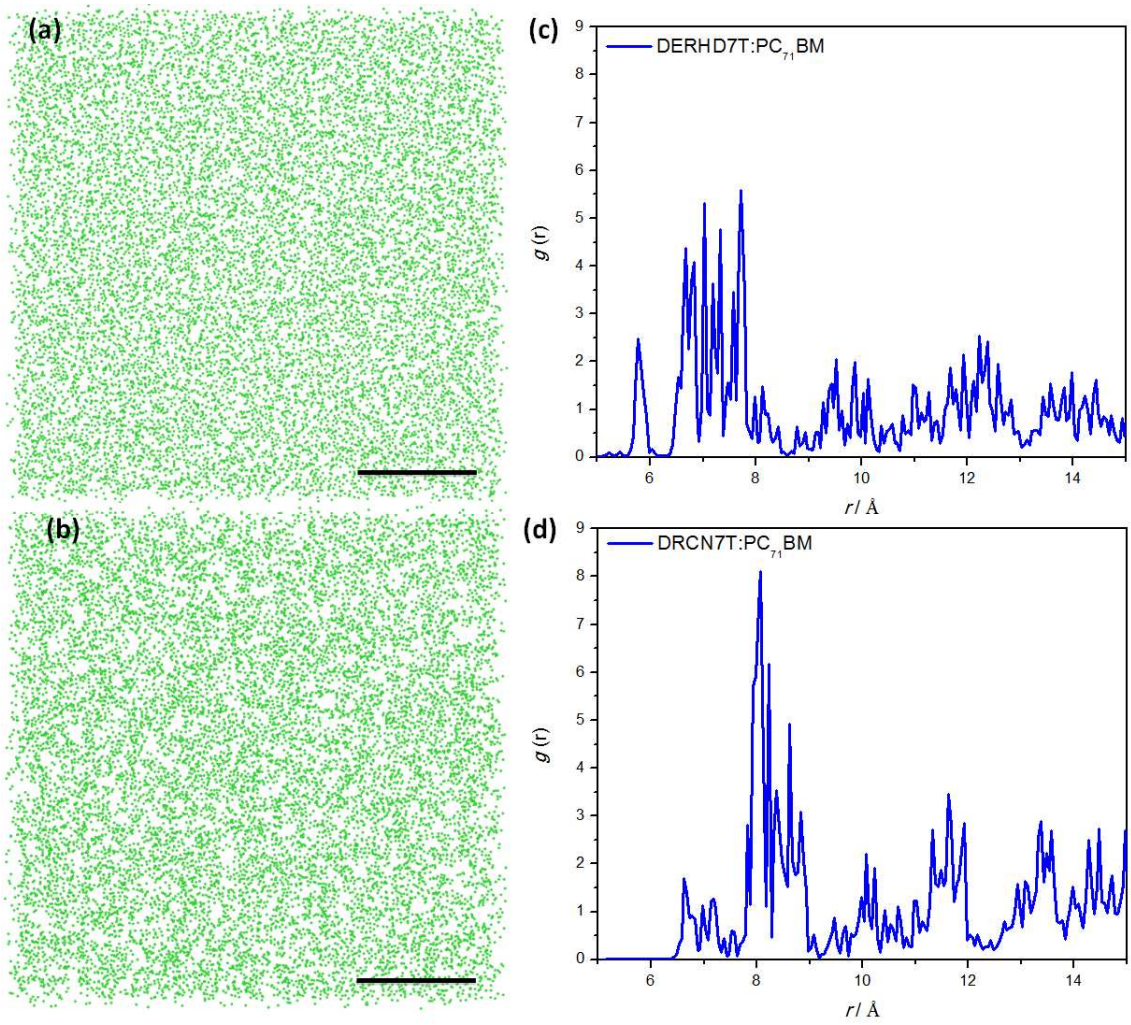

Figure S3. The sliced simulation snapshots (ca. 83 nm×83 nm×4 nm) with only end groups presented for **DERHD7T**:$PC_{71}BM$ (a) and **DRCN7T**:$PC_{71}BM$ (b). The scale bars are 20 nm. The RDFs for the end groups of **DERHD7T**:$PC_{71}BM$ (c) and **DRCN7T**:$PC_{71}BM$ (d) blends are also plotted.

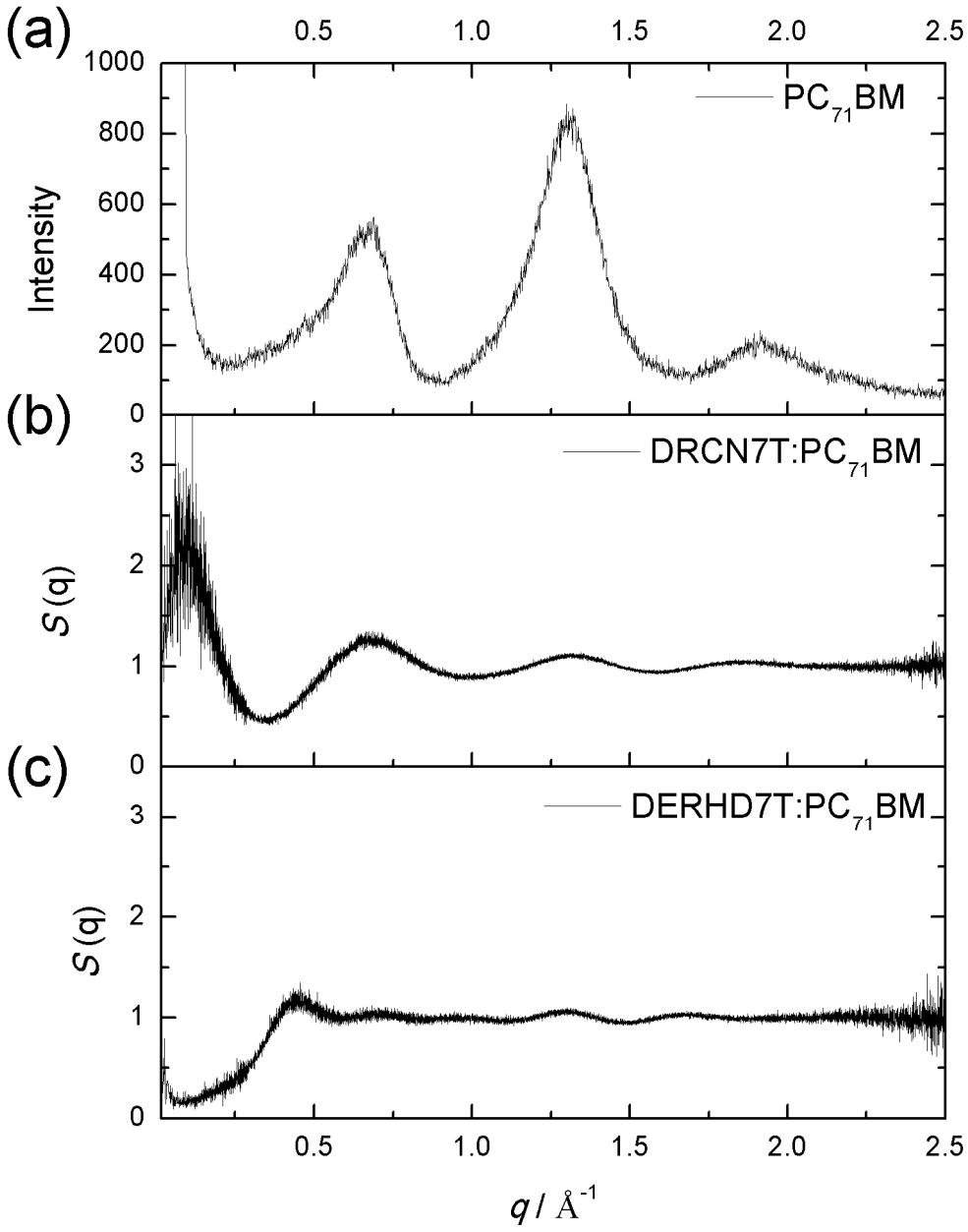

Figure S4. (a) The experimental powder X-ray diffractions of pure $PC_{71}BM$. The structure factors of $PC_{71}BM$ acceptors in **DRCN7T**:$PC_{71}BM$ (b) and **DERHD7T**:$PC_{71}BM$ (c) blends.

Table S2. Effective CG parameters of bonded interactions for **DRCN7T**.

Bond	r_0 [Å]	K [eV/Å^2]		
A-B bond	10.26	2.09E-02		
B-C bond	8.71	4.73E-02		
Angle	θ_0 [^{o}]	K_1 [eV/rad^2]	K_2 [eV/rad^3]	K_3 [eV/rad^4]
A-B-C	163.01	7.48E-01	1.45	0.66
B-A-B	185.22	2.35E-01	0.47	0.25
Dihedral angle	φ_0 [^{o}]	A [eV]	m	
C-B-A-B	91.06	9.21E-03	0.83	

Table S3. Effective CG parameters of bonded interactions for **DERHD7T**.

Bond	r_0 [Å]	K [eV/Å^2]		
A-B bond	9.98	2.04E-02		
B-C bond	8.49	5.71E-02		
Angle	θ_0 [°]	K_1 [eV/rad^2]	K_2 [eV/rad^3]	K_3 [eV/rad^4]
A-B-C	82.95	6.76E-01	1.55	0.75
B-A-B	166.26	7.98E-01	1.55	0.68
Dihedral angle	φ_0 [°]	A [eV]	m	
C-B-A-B	25.48	4.60E-03	0.71	

Table S4. Comparison of HOP values for different CG sites in the two systems.

Site	**DRCN7T**:$PC_{71}BM$	**DERHD7T**:$PC_{71}BM$
A	16.07	15.85
B	16.53	15.90
C	16.88	16.17
D	17.88	15.92

Reference List

1. Wang, Y.; Izvekov, S.; Yan, T.; Voth, G. A. Multiscale Coarse-Graining of Ionic Liquids. *J. Phys. Chem. B* **2006**, *110*, 3564-3575.

2. Noid, W.; Liu, P.; Wang, Y.; Chu, J. W.; Ayton, G. S.; Izvekov, S.; Andersen, H. C.; Voth, G. A. The multiscale coarse-graining method. II. Numerical implementation for coarse-grained molecular models. *J. Chem. Phys.* **2008**, *128*, 244125.

3. Hess, B.; Kutzner, C.; van der Spoel, D.; Lindahl, E. GROMACS 4: Algorithms for Highly Efficient, Load-Balanced, and Scalable Molecular Simulation. *J. Chem. Theory Comput.* **2008**, *4*, 435-447.

4. Van Der Spoel, D.; Lindahl, E.; Hess, B.; Groenhof, G.; Mark, A. E.; Berendsen, H. J. C. GROMACS: Fast, flexible, and free. *J. Comput. Chem.* **2005**, *26* , 1701-1718.

5. Berendsen, H. J. C.; van der Spoel, D.; van Drunen, R. GROMACS: A message-passing parallel molecular dynamics implementation. *Comput. Phys. Commun.* **1995**, *91*, 43-56.

6. Long, G.; Li, A.; Shi, R.; Zhou, Y. C.; Yang, X.; Zuo, Y.; Wu, W. R.; Jeng, U. S.; Wang, Y.; Wan, X.; et al. The Evidence for Fullerene Aggregation in High-Performance Small-Molecule Solar Cells by Molecular Dynamics Simulation. *Adv. Electron. Mater.* **2015**, *1*, 201500217.

7. Forester, T. R.; Smith, W. *Dl_Poly User Manual*. CCLRC, Daresbury Laboratory: Daresbury, Warrington, UK. **1995**.

8. Zhang, Q.; Kan, B.; Liu, F.; Long, G.; Wan, X.; Chen, X.; Zuo, Y.; Ni, W.; Zhang, H.; Li, M.; et al. Small-Molecule-Based Solar Cells with Efficiency Over 9%. *Nat. Photon.* **2014**, *9*, 35-41.

9. Wang, Y.; Voth, G. A. Tail Aggregation and Domain Diffusion in Ionic Liquids. *J. Phys. Chem. B* **2006**, *110*, 18601-18608.

10. Wang, Y.; Voth, G. A. Molecular Dynamics Simulations of Polyglutamine Aggregation Using Solvent-Free Multiscale Coarse-Grained Models. *J. Phys. Chem. B* **2010**, *114*, 8735-8743.

11. Chai, J. D.; Head-Gordon, M. Long-range corrected hybrid density functionals with damped atom-atom dispersion corrections. *Phys. Chem. Chem. Phys.* **2008**, *10*, 6615-6620.

12. Frisch, M. J.; Trucks, G. W.; Schlegel, H. B.; Scuseria, G. E.; Robb, M. A.; Cheeseman, J. R.; Scalmani, G.; Barone, V.; Mennucci, B.; Petersson, G. A.; et al. *Gaussian 09*, Revision B.01; Gaussian, Inc.: Wallingford, CT, **2010**.

13. Jeng, U. S.; Su, C. H.; Su, C. J.; Liao, K. F.; Chuang, W. T.; Lai, Y. H.; Chang, J. W.; Chen, Y. J.; Huang, Y. S.; Lee, M. T.; et al. A small/wide-angle X-ray scattering instrument for structural characterization of air-liquid interfaces, thin films and bulk specimens. *J. Appl. Cryst.* **2010**, *43*, 110-121.

14. Annapureddy H. V. R.; Kashyap, H. K.; Biase P. M. De; Margulis. C. J. What is the Origin of the Prepeak in the X-ray Scattering of Imidazolium-Based Room-Temperature Ionic Liquids? *J. Phys. Chem. B* **2010**, *114*, 16838.

15. Yan T.; Wang, Y.; Knox C. On the Structure of Ionic Liquids: Comparisons between Electronically Polarizable and Nonpolarizable Models I. *J. Phys. Chem. B* **2010**, *114*, 6905.